Research Square

Preprints are preliminary reports that have not undergone peer review.
They should not be considered conclusive, used to inform clinical practice,
or referenced by the media as validated information.

Glucose metabolism of camel reveals differences in glucose adaptation modes in different tissues

Yanru Zhang

yanru1964@163.com

Hainan Vocational University of Science and Technology

Yu Ling

Inner Mongolia Agricultural University

Research Article

Keywords: Intolerance, ROS, Oxidative stress, Antioxidant, High blood glucose

Posted Date: May 30th, 2026

DOI: https://doi.org/10.21203/rs.3.rs-9471788/v1

License: This work is licensed under a Creative Commons Attribution 4.0 International License.
Read Full License

Additional Declarations: No competing interests reported.

Abstract

Introduction: Camels have the physiological characteristics of high blood sugar. If the blood glucose concentration of humans is comparable to that of camels, humans will suffer cell damage due to sugar intolerance.

Aims: This study aims to study the mechanism of camel sugar tolerance in multiple tissues.

Materials and Methods: We applied RNA-seq and protein mass spectrometry to five tissue types.

Results: We found that there are obvious differences in the expression profiles of different organs. The analysis showed that the glucokinase (*GCK)* is not expressed in the liver for self-protection. The lack of an antioxidant (blood uric acid) in the blood of camel is due to the absence of expression of solute carrier family 2 member 9 (GLUT9) in the kidney, whereas the expression of secreted antioxidant proteins in the renal cortex is an alternative route to the loss of blood uric acid. Heat shock protein is the protective protein in both the renal cortex and the muscle. Low expression of transporters reduces sugar intake and protects pancreatic cells.

Conclusions: This study clarifies the gene expression mechanism of sugar tolerance in different tissues of camel and provides a reference for human sugar intolerance research.

Introduction

Camels have high blood glucose levels compared to humans and other mammals in long-term evolution. In contrast, when human blood glucose levels are comparable to normal camel blood glucose levels, diabetes is imminent or may be induced. Research has indicated that if the blood glucose concentration is too high in humans, it will lead to an increase in Reactive oxygen species (ROS) within cells[1], induce apoptosis[2], including apoptosis of islet β-cells[3–5], and ultimately trigger tissue destruction in organs including the pancreas, resulting in diabetes[4].

The domesticated Bactrian camel (*Camelus bactrianus*), the dromedary camel (*Camelus dromedarius*), and the wild Bactrian camel (*Camelus ferus*) belong to the genus Camelus[6, 7]. With its tolerance for cold and drought, the domesticated Bactrian camel used to be the main mode of transportation on the Silk Road[8]. Current research shows that the camel has a series of unique physiological characteristics, including adapting to extreme water shortages[9], salt tolerance, a special immune system, and high blood glucose levels[10]. Mammals especially have various ranges of blood glucose concentration (BGC). BGC ranges from 3.5–5.0 mmol/L in monogastric animals, including 2.3–2.4 mmol/L in cows (*Bos taurus*), 2.4–4.5 mmol/L in sheep (*Ovis aries*), and 2.7–4.2 mmol/L in goats (*Capra hircus*)[11, 12]. In humans, the normal range of BGC is 3.8–6.1mmol/L. Impaired fasting glucose (IFG) is defined as fasting plasma glucose level from 6.1 mmol/L to 6.9 mmol/L (World Health Organization) and from 5.6 mmol/L to 6.9 mmol/L (American Diabetes Association) in humans [13]. An IFG level classified as “pre-diabetes” predicts a high risk of future diabetes[14, 15]. Fasting plasma glucose level ≥ 7.0 mmol/L is

defined as diabetes mellitus in humans. Human cells are intolerant to hyperglycemia. Interestingly, the BGC range of genus *Camelus* is 6–8 mmol/L and basal glucose value is 7.1 ± 0.3 mmol/L [11, 12]. The normal value of blood glucose in camel spans the range of IFG and diabetes in humans. However, it remains unknown how camels can metabolize at high blood glucose levels. Although a previous report showed that hyperglycemia in camels provides support for maintaining both osmotic conditions and body fluid homeostasis in arid deserts [16], it did not elucidate how camels can handle the adverse effects of high glucose.

In this study, we investigate the mechanisms behind hyperglycemic adaptation using transcriptomics and proteomics. The liver and muscles as the main organ for storing sugar, the pancreas secretes insulin and glucagon to regulate blood sugar, and the kidneys reabsorb glucose, so we sequenced the transcriptomes of liver, muscle, renal cortex, renal medulla, and pancreas. We also gained proteome of renal cortex and renal medulla. The study characterized glucose adaptation strategy within main tissues.

Materials and Methods

2.1 Animals

We observed three Bactrian camels(*Camelus bactrianus*) living under natural conditions with free access to food and water. The camels were fasted for 12 hours before termination by electric shock to obtain fasting blood glucose levels. The renal cortex, renal medullar, liver, pancreas, and muscle samples were taken from two males (age: six years, weight: 361 kg; age: seven years, weight: 383 kg) and one female (age: six years, weight: 370kg), and the samples are frozen immediately in liquid nitrogen and stored at -80°C. We also obtained 30 normal camel blood samples and 30 urine samples from 15 males and 15 females (age: 6–8 years, weight: ~ 390kg).

The animals were privately owned by a local farm in Inner Mongolia, and informed consent was obtained from the owner for the use of animals in this study.

2.2 RNA-seq sample collection and preparation

RNA degradation and contamination were monitored on 1% agarose gels. RNA purity was checked using the Nano Photometer spectrophotometer. RNA integrity was assessed using the RNA Nano 6000 Assay Kit of the Bioanalyzer 2100 system (Agilent Technologies). A total of 3 μg RNA per sample was used as input material for RNA sample preparations. mRNA was purified from the total RNA using poly-T oligo-attached magnetic beads. Fragmentation was carried out using divalent cations under elevated temperature in NEBNext First Strand Synthesis Reaction Buffer (5X). First strand cDNA was synthesized using random hexamer primers and M-MuLV Reverse Transcriptase (RNaseH). Second strand cDNA synthesis was subsequently performed using DNA Polymerase I and RNase H. Sequencing libraries were generated using NEBNext Ultra RNA Library Prep Kit for Illumina (NEB) following manufacturer's recommendations and were sequenced on an Illumina Hiseq platform, and 125 bp paired-end reads were generated.

2.3 RNA-seq Data Analysis

Data in fastq format were processed through in-house perl scripts. Reference genome and gene model annotation files were downloaded from genome website directly(https://www.ncbi.nlm.nih.gov/genome/10741). A reference genome index was built using Bowtie v2.2.3 [17] and paired-end clean reads were aligned to the reference genome using TopHat v2.0.12 [18] with default parameters. HTSeq v0.6.1 [19] was used to count the reads numbers mapped to each gene. Prior to differential gene expression analysis, for each sequenced library, the read counts were adjusted by the 'edge' R program package [20] through one scaling normalized factor. Differential expression analysis of two conditions was performed using the 'DEGSeq' R package (1.12.0) [21]. The P-values were adjusted using the Benjamini & Hochberg method. A corrected P-value of 0.005 and log2 (Fold change) of 1 were set as the threshold for significantly differential expression. We used KOBAS software to test the statistical enrichment of differentially expressed genes in pathways (http://www.genome.jp/kegg/).

2.4 Protein Mass Spectrometry

Experimental tissue sampling

The fresh renal cortex and renal medulla derived from three camels was mixed in the same mass (330 mg) into powder for protein extraction. Proteins for SDS electrophoresis were extracted.

Protein gelatinysis

The whole protein strip was cut from top to bottom into 10 components, each of which was cut into pieces of about 1 mm3 with a knife and placed in 10 EP tubes, respectively; 500 μl of pure water was added to each tube. Wash for 10 min and repeat twice. 500 μl of acetonitrile was added to each tube and dehydrate for 10 min. 10 mM DTT was added and incubated at 56℃ for 1 h. Subsequently, 55 Mm IAM was added to block the cysteines, and incubate for 1 h in the darkroom. 25 mM NH4HCO3 in DTT at a final concentration of 10 mM was incubated at 56℃ for 1 h; 25 mM NH4HCO3 with an IAM final concentration of 55 mM was added and the dark room was allowed to stand at room temperature for 45 min. 500 μl of 25 mM NH4HCO3 was added to each tube. Wash for 10 min and repeat twice. 500 μl of acetonitrile was added to each tube and dehydrate for 10 min; Dry the acetonitrile. 50μl of 0.01μg/μl Trypsin was added. 37℃ overnight. Add 5% formic acid (FA) to terminate the reaction.

Peptide extraction

Using 50% acetonitrile 200ul 0.1% formic acid extraction once; Using 100% acetonitrile 200ul 0.1% formic acid extracted twice; Collect all the supernatants and vacuum dry.

LC-ESI-MS/MS analysis based on Triple TOF 5600

Each of the drained components was reconstituted with buffer A (2% ACN, 0.1% FA) to a concentration of about 0.5 μg/μl, centrifuged at 20000 g for 10 min, and insoluble materials were removed. Each of the fractions was loaded with 10 μl (about 5 μg protein) and subjected to reverse phase separation by a nanoHPLC of LC-20AD model (Shimadzu, Japan). The reversed-phase column used was a C18 column consisting of two sections: a 2 cm length injection section with an internal diameter of 200 μm and a 10 cm length elution separation section with an internal diameter of 75 μm. The separation procedure was as follows:(1) 4 minutes at a flow rate of 15 μl/min and then 44 minutes at a flow rate of 400 nl/min with a wash gradient from 2% to 35% for buffer B (98% ACN, 0.1% FA). (2) linear elution from 35% to 80% for 2 minutes. (3) wash column with 80% buffer B 4 minutes, buffer A wash column for 1 minute.

The machine used was a Triple TOF 5600 (AB SCIEX, Concord, ON) with a Nanospray III source (AB SCIEX, Concord, ON) as an ion source and a emitter (New Objectives, Woburn, MA). When data is collected, the machine parameters are set as follows: Ion source spray voltage of 2.5kv, nitrogen pressure of 30psi, spray pressure of 15psi, spray interface temperature of 150 degrees Celsius; Scan mode is reflective mode with a resolution ≥ 30,000; survey scans were acquired in 250 ms and as many as 30 product ion scans were collected if they exceeded a threshold of 120 counts per second (counts/s). Total cycle time was fixed at 3.3 s.

The second quadrupole of the transmission window is set to 100Da for 100%; pulsed RF frequency of 11kHz; detector detection frequency of 40GHz; each scan of the particle signal were recorded four channels were merged into four data were recorded; ion fragmentation Of the energy is set to 35 ± 5eV; the parent ion dynamic exclusion is set to: within half the peak time (18s), the same mother ions fragmentation no more than 2 times.

Data analysis

Protein identification Using MASCOT 2.3.02 software [22] identified proteins. The parameters were as follows: MS/MS Ion Search as Type of search, Trypsin as Enzyme, 1 as Max Missed Cleavages, Monoisotopic as Mass Values, 0.05Da as Peptide Mass Tolerance, 0.1Da as Fragment Mass Tolerance, Carbamidomethyl (C) as Fixed modifications, Gln->pyro-Glu (N-term Q),Oxidation (M),Deamidated (NQ) as Variable modifications, ESI-QUAD-TOF as Instrument type, LuoTuo_BGI(20251 sequences) as Database. Charge states should include + 2, +3, and + 4. To reduce the identification of false-positive peptides, the FDR of the screened peptides was less than 0.01. And each confident protein identification involved at least one unique peptide. The mass spectrometry proteomics data have been deposited to the ProteomeXchange Consortium via the PRIDE [23] partner repository.

2.5 Real time quantitative polymerase chain reaction

Real time quantitative PCR (qPCR) with SYBR Green dye was used to validate RNA-Seq data with poly(A) RNA prepared as described in the cDNA synthesis section above. Real time qPCR was carried out on a Roche LightCycler 480 with a 20 μl reaction volume containing 1 μl of cDNA, 2X SYBR® Premix Ex Taq™ (Tli RNaseH Plus) (TAKARA, P/N RR420A), 5 picomoles each of forward and reverse primers. The reaction was done in three replicates for each of the 34 ORFs selected from high confidence list. The

standard curve preparation was performed under the same conditions, but with a dilution series of 0.01, 0.10, 1.0 and 10 ng of genomic DNA instead of cDNA; a negative control was also performed using water instead of cDNA. qPCR was performed with the following PCR protocol: 95℃ for 5 min; 59 cycles of 95℃ for 10 seconds, 55℃ for 20 s, and 72℃ for 30 seconds. Lastly, a ramp from 65℃ to 95℃ at 2.5℃/ s was used to determine melting curves. The Crossing Point (CP) values were determined with the 2nd derivative max method in the supplied Roche software. These were then exported, and data was handled in R (http://www.r-project.org/).

2.6 Statistics

Student's t-test was used to analyze two independent experiments. P values of less than 0.05 is considered statistically significant.

2.7 Detection of physical and chemical indicators

30 camels blood samples were used to measured serum uric acid levels using automatic biochemical analyzer (BS-800) from Mindray (Shenzhen, China) with default parameter settings. Thirty camel urine samples were obtained to detect glucose levels using URIT-330 from URIT (Guilin, China) with default parameter settings. Automatic biochemical analyzer (BS-800) from Mindray (Shenzhen, China) was used to detect blood sugar levels in blood samples of the 30 camels with default parameter settings.

Results

3.1 Tissues Exhibit Different Metabolic Characteristics under High Blood Glucose Levels

To study how the tissues adapt to physiological blood glucose levels (6-8mmol/L) [11, 12] that is higher than that in human (3.8-6.1mmol/L), we sampled the tissues of liver, renal cortex, renal medulla, muscle and pancreas from 3 adult camels living wild condition and abstracted these tissues RNA, then sequenced them using Illumina platform. Renal cortical protein and renal medulla protein were extracted for PMS. We analyzed the transcriptional and protein profiling of main glucose metabolism tissues.

Using a significance level of |log2 (Fold Change)| > 1 and q-value < 0.005, we analyzed a large number of differentially expressed genes among the tissues (Fig. 1A; Fig. S1), which presented expression differences among the tissues in camel. We obtained 15 genes that are highly expressed in five tissues (Table. S1). Several genes reported previously as having specific expression in relevant human tissues displayed significantly high expression levels in the counterparts of camels, such as the genes encoding albumin (*ALB*) [24], haptoglobin (*HP*), apolipoprotein C (*APOC*) [25], and selenoprotein P (*SEPP1*) [26] in the liver; uromodulin (*UMOD*) [27, 28], ferritin (*FT*) [29], enoyl CoA hydratase (*ECHS1*) [30], and clusterin (*CLU*) [31] in the kidney; chymotrypsin C (*CTRC*) [32], chymotrypsin-like elastase family, member 3B (*CELA3B*) [33], carboxypeptidase A1 (*CPA1*) [33], phospholipase A2, group IB (*PLA2G1B*) [34], carboxyl ester lipase (*CEL*) [35, 36], serine peptidase inhibitor, and Kazal type 1 (*SPINK1*) [37] in the pancreas; and

ankyrin repeat domain 1 (*ANKRD1*) [38], myosin light chain, phosphorylatable, fast skeletal muscle (*MYLPF*) [39], creatine kinase (*CKM*) [40], troponin C type 2 (TNNC2) [41], myoglobin (*MB*) [42], filamin C, gamma (*FLNC*) [43], and kelch-like family member 41 (*KLHL41*) [44] in the muscle (Table. S1). Interestingly, we also detected a markedly high expression of glutathione peroxidase 3 (*GPX3*) (fragments per kilobase per million mapped fragments(FPKM) = 21081) in the renal cortex, which was a hydrogen peroxide scavenger in the blood [45] (Table. S1). Simultaneously, *HSPB1*, *HSPA6*, and *CRYAB* have been reported to encode the chaperones [46–49], which were significantly expressed in the muscle (Table. S1).

Functional enrichment analyses of all up-regulated genes in a tissue relative to the other four tissues revealed the enrichment of metabolic pathways, including PPAR signaling pathway, starch and sucrose metabolism in the liver (Fig. 1B), biosynthesis of amino acids and carbon metabolism in the renal cortex (Fig. 1C), and pancreatic secretion in the pancreas (Fig. 1D).

Hierarchal clustering performed with a log10 (FPKM + 1) value in gene expression for the five tissues revealed that renal medulla and renal cortex cluster closely together, whereas liver and muscle cluster closely together (Fig. 1E). The pancreas and kidney are less associated with this cluster and the species of highly expressed genes are less in the pancreas compared to other tissues (Fig. 1E). Notably, there is only a moderate correlation among the different tissues, indicating that there are obvious gene expression differences in tissues in a high glucose environment (Fig. S2).

3.2 Tissues Differentially Expressed Genes in Glucose Metabolism Pathway

To investigate differences of glucose metabolic ability of tissues in camel, we observed the expression of glycolysis-related genes in the five tissues. The hexokinase family catalyzes the first step of glycolysis which is also a rate-limiting step [50]. The hexokinase family consist of four members, hexokinase 1 (*HK1*), hexokinase 2 (*HK2*), hexokinase 3 (*HK3*) and glucokinase (*GCK*), and converts glucose to glucose 6-phosphate (G-6-P) [51]. We also focused on ketohexokinase (*KHK*), which catalyzes the conversion of fructose to fructose-1-phosphate; the product of KHK is the first enzyme in a specialized pathway to catabolize dietary fructose [52]. We found that *HK1*, *HK2*, and *KHK* were expressed in the muscle, *KHK* and *HK1* in the pancreas; *KHK* and *HK1* in the renal cortex, and *HK1*, *HK2* and *KHK* in the renal medulla (Fig. 2A). The major genes expressed in liver were *KHK*, *HK1* and *HK3* without *GCK* (Figs. 2A, 2B and 5A; Table. S2). Tissues selectively uses different rate-limiting enzymes at the first step of glycolysis. Our findings indicate that camels' livers did not express *GCK*. It has been reported that some vertebrates also lack hepatic GCK activity [53]. This means that camel liver utilize *HK1* and *HK3* instead of *GCK* for the first step of glycolysis.

Furthermore, we analyzed genes involved in glucose metabolic pathway (HK & KHK pathway and auxiliary transport route) in the five tissues. The genes involved in the pathways showed a significantly high expression in the renal cortex comparing to the pancreas, including solute carrier family 5 member

2(*SLC5A2)* encoding SGLT2, *HK1*, *KHK*, glucose-6-phosphate isomerase (*GPI)*, phosphofructokinase (*PFK)*, glucose-6-phosphatase catalytic subunit (*G6PC)* encoding G6Pase, aldolase (*ALDOA)*, triosephosphate isomerase 1 *(TPI1)*, Aldo-keto reductase family 1 member B *(AKR1B1)*, solute carrier family 2 member 2 *(SLC2A2)* encoding GLUT2, fructose-bisphosphatase *(FBP)* and sorbitol dehydrogenase (*SORD)*, solute carrier family 12 member 1 *(SLC12A1)* encoding NKCC2, *and* sodium/potassium-transporting ATPase *(ATP1A1, ATP1B1)* (Figs. 2C,5B). This scenario may reflect the organ's physiological function, which relates to a large number of nephrons in the renal cortex functioned as reabsorption of glucose and ion. The result indicates that all of the glucose metabolic pathways in camel's renal cortex, renal medulla, liver and muscle are more active than the pancreas (Fig. 2C; Table. S2). Interestingly, the low expression of genes in the pancreas in this pathway is most evident in the five tissues (Figs. 2C-2G). Aldolase (*ALDOA*) is of high expression in the pancreas (pancreas *v.s.* liver) (Figs. 2D and 5A), but *ALDOB*, an isoenzyme of *ALDOA* has a significantly higher expression in the liver (Figs. 2D and 5A). However, we only detected the high expression of solute carrier family 37 member 4 (*SLC37A4)* encoding G6PT1 in the pancreas (pancreas v.s. muscle & pancreas v.s. renal medulla) (Figs. 2E-2F) and non-differential expression of *SLC37A4* in the pancreas (pancreas v.s. liver & pancreas v.s. renal cortex). *SLC37A4* is responsible for the sugar balance in cells [54]. The result indicated that the glucose metabolism activity in pancreas was weaker than other four tissues, but the ability of maintaining glucose homeostasis in cells was stronger than the muscle and the renal medulla, like the liver and the renal cortex.

We quantitatively analyzed the major genes mentioned above in the renal cortex, the liver and the pancreas by qPCR. The results confirmed the conclusions of transcriptome data analysis (Figs. S3A-S3C). Furthermore, we detected protein expression of the above genes in the renal cortex by PMS. The corresponding proteins are also presented in the renal cortex (Table. S3).

3.3 Differentially Expressed Antioxidant Genes and HSP Genes in tissues

The role of enzyme antioxidant system is responsible for eliminating excessive free radicals generated by Oxidative stress [55, 56]. RNA-seq results showed that the expression of antioxidant genes from the pancreas, specifically *IDH1* and *SOD1* (in cytoplasmic matrix)[57], *IDH2* and *SOD2* (in mitochondria)[57], as well as *CAT, GPX1*, and *GSR*, were down-regulated compared to the other four tissues (Fig. 3A; Table. S2, Figs.S3D-S3H). The low expression of antioxidant genes in the pancreas is consistent with the previous studies in humans [58, 59], indicating camel's pancreas has weak antioxidant capacity like humans. In contrast, the genes in the renal cortex display remarkably high expression (Figs. 3A and 6). Antioxidant proteins (SOD1, SOD2, SOD3, CAT, GSR, IDH1, IDH2, GPX1 and GPX3) were detected in renal cortex by protein mass spectrometry, except for GPX4 (Table. S3). It reflects that the renal cortex needs more antioxidants to clean ROS generated by high glucose.

We also analyzed the expression of HSP family genes in the tissues of camels under high glucose conditions, especially the subfamilies functioned as molecular chaperones including HSP90, HSP70,

HSP60 [60], HSP40, and HSP20 [61]. We found that the expression pattern of the renal medulla was similar to the renal cortex (Fig. 3B). In addition, the muscle, liver, renal cortex and renal medulla highly expressed different members of HSP, but the pancreas had a low expression of HSP members (Fig. 3B, Table. S2, Figs.S3I-3K). The members of chaperone genes from subfamilies exhibit an evident difference between renal cortex and pancreas (Fig. 3C, underline), such as HSP90 subfamily (*HSP90AA1, HSP90B1*, and *TRAP1*), HSP70 subfamily (*HSPA2, HSPA8, HSPA9*), HSP60 (*CCT6A, HSPD1*), HSP40 subfamily (*DNAJA3, DNAJB1, DNAJB11, DNAJC13, DNAJC19, DNAJC22, DNAJC6, and DNAJC8*), and HSP20 subfamily (*GRPEL1, CRYAB, HSPB1, and HSPB8*). The difference in HSPs between muscle and pancreas is even more apparent (Fig. 3D). This indicates that the pancreas demands fewer HSPs than other four tissues, and the renal cortex and the muscle need more HSPs(Table. S3).

3.4 Members of SLC family as gated channels are unevenly distributed among tissues

To explore the differences in glucose uptake capacity among different tissues, we focused on all of the gene expression related to glucose transporter, including the SLC2 family of membrane transporters (Facilitative GLUT transporter family), glucose transport families SLC5 (Sodium glucose cotransporter family), the SLC45 gene family of putative sugar transporters (Putative sugar transporter family) and the glucose transport families SLC50 (Sugar efflux transporters). There were differences in the SLC expression patterns among the tissues. The renal cortex and the renal medulla converged into one category because of the high expression patterns, while the pancreas and the liver displayed a low abundance of SLC family (Fig. 4A; Table. S2, Figs. S3L). However, the abundance of differently expressed genes from SLC family in the pancreas is lower than that in the liver (Fig. 4B, Figs. S3B). This indicates that the pancreas reduces expression of SLC families. Furthermore, *SLC5A2*, a member of SLC family, that is mainly responsible for the reabsorption of urinary glucose along kidney proximal tubules in rats [62], is highly expressed in the renal cortex (renal cortex v.s. pancreas) (Fig. 4B, Figs. S3L,Table.S3). We measured camels' urine glucose content and fasting plasma glucose value from 30 individuals. The test result of urine glucose content was negative (Table. S4). The average fasting plasma glucose value was 6.9 ± 0.63 mmol/L (Table. S4). This indicates that the camel reabsorbs all of the glucose in crude urine without removing it from the body, despite its blood glucose level is in the range of IFG for humans.

3.5 Kidney is as a Main Organ to Maintain Extracellular Redox Balance

Blood redox homeostasis directly affects the peripheral tissues. Uric acid is one of the antioxidants in non-enzymatic antioxidant systems in blood and its role is to neutralize excess ROS to reach a redox state of equilibrium [63].

The uric acid content of camel's serum was 2.93 ± 1.70 μmol/L (n = 30) on average (Table. S4). The normal range of serum uric acid is 280.50 μmol/L in humans (n = 30). The uric acid content in camels' blood is much lower than that in humans' blood (p = 3.19587E-66). Furthermore, we showed that *SLC2A9*

mRNA was not transcribed in the camel kidney (Table. S2) and the corresponding protein (GLUT9) was not detected in the kidney (Table. S3). GLUT9 is expressed in the proximal tubules of the kidneys and is responsible for reabsorbing uric acid from crude urine back into the bloodstream [64]. It is likely that the lack of GLUT9 results in kidneys not reabsorbing uric acid back into the blood, which in turn leads to lower serum uric acid content.

However, we observed a significant expression of the exocrine-type antioxidants in the renal cortex, *SOD3* and *GPX3*, which were significantly higher than the other four tissues (Fig. 3A, Table. S5, Figs. S3D-S3E). Both proteins playing a role of scavenging oxidants in blood were identified in the renal cortex (Table. S3).

Discussion

The study of the mechanism of adaptation to hyperglycemia in a non-artificial model of high glucose animals was first performed in the multi-tissue and multi-level experiment. We applied RNA-seq to study glucose metabolic characteristics of each type of tissue in camels. Furthermore, we identified the full spectrum of proteins of the kidney to determine their main function for hyperglycemia metabolism. However, each of tissues of camels has formed unique metabolic pathways.

In liver, several reports indicated that *GCK* is specifically expressed in human [65–67]. Unlike the previous studies, we found that the first glycolytic rate-limiting enzymes in camel's liver are *HK1* and *HK3* instead of *GCK*. *GCK* is not inhibited by the negative feedback regulation of metabolites (D-Glucose 6-phosphate, G-6-P) in mammals [65], meaning that under conditions of sufficient glucose, *GCK* will convert glucose to G-6-P in the cells continuously, whereas the accumulation of metabolites (G-6-P) leads to the accumulation of ROS and is thought to be the source of oxidative stress [58]. Other members of the HK family differ from *GCK*. They are regulated by G-6-P [51], which inhibits the activity of *HK* and reduces the accumulation of G-6-P to avoid cell damage. Furthermore, we found that another way to provide energy for the cell was though the KHK pathway. KHK produce D-Fructose 1-phosphate, not to cause damage to cells. Therefore, the findings suggest that giving up the GCK in liver is a self-protecting option to avoid the accumulation of G-6-P, and the camel's liver has evolved its pathway that reduces possible cell damage (Fig. 5A).

In renal cortex, we observed that genes in the HK and KHK pathways and the auxiliary transport route exhibited high expression. Studies have shown that SGLT2 mediating glucose reabsorption in the proximal tubule [68] is induced at high glucose [69]; GLUT2 contribute to glucose export into the bloodstream [70, 71]. ATPase maintain the electrochemical gradients of Na and K ions across the plasma membrane [72]. Increased NKCC2 improve glucose disposal in mice [73]. G6Pase catalyzes the hydrolysis of G-6-P to glucose [74]. G6PT1 regulates glucose-6-phosphate transport from the cytoplasm to the lumen of the ER [54]. G6PT1 is a key enzyme in maintaining glucose homeostasis [54, 74]. Active metabolism of the above proteins in the renal cortex helped camels to save and use glucose, indicating the renal cortex carried out a strong glucose metabolism (Fig. 5B).

We also found a high expression of antioxidant enzymes in the renal cortex and the low expression in the pancreas. GSR is a central enzyme in cellular antioxidant defense, and reduces oxidized glutathione disulfide (GSSG) to the sulfhydryl form (GSH) [75], which is useful for GPX converting H_2O_2 to H_2O; IDH serves as a significant role in NADPH production, which assists GSR to convert GSSH to GSH. SOD is responsible for converting superoxide radicals to molecular oxygen and hydrogen peroxide H_2O_2 [57]. CAT converts the reactive oxygen species hydrogen peroxide to water and oxygen[76]. GPX catalyzes the reduction of organic hydroperoxides and H_2O_2 [77]. Finally, the collaboration of these enzymes contributes to ROS clearance. Furthermore, studies have shown the increased expression of these enzymes within high glucose environments [78]. Our data suggest that the renal cortex needs more antioxidants to convert superoxide radicals and hydrogen peroxide to water and molecular oxygen, helping the renal cortex adapt to high glucose (Fig. 6).

Interestingly, we found high levels of multiple chaperones presented in the renal cortex. Chaperones from the HSP subfamily play major roles in mediating protein refolding, tissue protection, tissue repair, and protein homeostasis [79]. There is a widespread clinical interest in the protective role of the HSP family against a variety of diseases, including obesity, insulin resistance, and diabetes [79]. Specially, the HSP70 subfamily and the HSP90 subfamily are molecular chaperones expressed constitutively under normal conditions to maintain protein homeostasis and they are induced when subjecting to environmental stress [80, 81]. More specifically, HSPA8 (HSP70 subfamily) functions in a diverse set of processes, including protein folding[82]; HSP90AA1, HSP90B1 [83], and TRAP1 (HSP90 family) are induced by the stress [82, 84, 85]. Studies have also shown that high glucose significantly upregulated mRNA and protein expression of HSP70 and HSP90 [85]. Moreover, the HSP60 subfamily can promote folding and assembly of newly imported proteins [86, 87], stabilize proteins destined for re-export to intermembrane space [88], bind heat-denatured mitochondrial proteins and prevents aggregation [89]. The HSP40 subfamily acting as co-chaperones help the HSP70 subfamily achieve chaperone functions as well [90, 91]. There is evidence indicating that HSP may protect eukaryotes from the toxic effects of ROS [92] under high glucose conditions. Our data suggest that the remarkable upregulation of chaperones in the renal cortex is necessary, which could avoid the accumulation of misfolded protein to lead to cell damage in the cytoplasmic matrix and ER (Fig. 6).

We found a significantly high expression of *HSPB1*, *HSPA6* (HSP70 subfamily), and *CRYAB* (HSP20 subfamily) in muscle. Under stress, these members from the HSP20 subfamily are overexpressed to counter protein aggregation and apoptosis [93, 94]. HSPB1 (HSP20 subfamily) has chaperone and antiapoptotic activities [46]. For example, HSPB1 can help protein folding under oxidative stress [95]. In fact, the protective activity of HSPB1 against H_2O_2-mediated cell death in the murine L929 fibroblast has been observed[95]. The rise of HSPB1 levels has also been discussed under high glucose levels [96]. It has been reported that *HSPA6* is induced under high levels of stress[97]. Moreover, high glucose levels will increase the expression of *CRYAB* [98], and *CRYAB* is up-regulated by ER stress [99]. Therefore, the muscle might use chaperones to protect intracellular proteins from OS and ER stress.

We identified the low expression of the glucose transporter in the pancreas. It is also likely that reducing the uptake of glucose, as a defensive approach, avoids OS produced by glucose accumulation in the pancreas. However, in the kidney, SGLT2 expressed in the proximal renal tubules accounts for about 90% of the reabsorption of glucose from crude urine [62, 100, 101]. High expression of SGLT2 in camel's renal cortex and no glucose in camel's urine suggest that camels' kidneys reabsorb glucose to avoids the loss of sugar in a resource-deprived desert. Therefore, it is possible that camels express the SLC family differently to distribute blood glucose to various tissues. Differentially expressed SLC family members meet the kidney sugar metabolism needs, while avoiding damage to the pancreas caused by high glucose levels.

It was reported that elimination of ROS by serum uric acid is one way for human to maintain redox homeostasis in blood [63, 102, 103], and uric acid improves glucose-driven oxidative stress in human [104]. Unlike previous studies, we observed significantly low uric acid in the camel's blood. It is likely that the camels' kidneys lack GLUT9. Consequently, camels do not use serum uric acid to balance ROS in a blood vessel.

In addition, we also identified the high expression of SOD3 and GPX3 in the renal cortex. The enzymes were reported previously to be processed in the kidney and released into the bloodstream to neutralize excessive ROS [45, 105–107]. A high level of SOD3 expression has been observed in glomerular capillary [108]. Overexpression of SOD3, contributing to overcome of oxidative stress and reducing ROS, has been shown to prevent diabetes mellitus [109]. Increased GPX3 may protect cardiomyocytes from oxidative stress caused by hyperglycemia [110]. We believe that, despite the lack of serum uric acid, exocrine enzymes (SOD3 and GPX3) from the kidney can also maintain the redox homeostasis of blood. It is more noteworthy that the human pancreas has an enhanced affinity for circulating SOD3, or translating the SOD3 message more efficiently than other tissues [111]. It is possible that both enzymes ensure the pancreas to be free from free radical attack in the case of less synthetic antioxidant genes and HSP family genes, indicating that the kidney not only protects own intracellular redox homeostasis, but also improves the blood environment for other tissues, such as the pancreas (Fig. 6).

Conclusions

We determined the high glucose-induced adaptation mechanism in the transcriptome and PMS of the major tissues of camels. One key finding is that adaptation to hyperglycemia entails a markedly different expression of genes involved in glycolysis, antioxidant enzymes, HSP and SLC proteins among tissues. These proteins are organized according to the distinctive needs of the tissues. We found ways to tolerate hyperglycemia in camels. One is scavenging ROS from blood by SOD3 and GPX3 produced in the renal cortex. The other is expressing highly antioxidant proteins and HSPs in the kidney, escaping *GCK* in the liver and reducing the expression of SLC in the pancreas (Fig. 7). These ensure camels can adapt to high glucose.

Declarations

This work was supported by the Double First-Class Fund for Introducing Outstanding Doctoral Talents in Genomics and Biotechnology (Grant No. DC2000001589) from the 2020 Fiscal Year.

Funding

This work was supported by the Double First-Class Fund for Introducing Outstanding Doctoral Talents in Genomics and Biotechnology (Grant No. DC2000001589) from the 2020 Fiscal Year.

Statement of Ethics

Camels are domestic animals locally, similar to pork as the main food source for humans. Because the method of anesthesia may cause changes in tissue metabolism and affect the experimental data, this study used electric shock to instantly kill the animals, and strictly followed the experimental animal standards. The use of experimental animals and related procedures involved in the experiment were approved by Laboratory Animal Welfare and Ethics Committee of Inner Mongolia Agricultural University (NO. NND2021085).Informed consent was obtained from the camel owner for the use of animals in this study.

Disclosure Statement

The authors declare that they have no competing interests. Yanru Zhang is responsible for data collection, and Yu Ling is in charge of data analysis and article writing.

Availability of data and materials

The accession number for the RNA-seq data reported in this paper is SRA: PROJNA416060. The accession number for the mass spectrometry proteomics data is PRIDE: PXD009141. Data is publicly available.

Abbreviations

Not applicable.

Ethics approval and consent to participate

The use of animals was approved by the Laboratory Animal Welfare and Ethics Committee of Inner Mongolia Agricultural University (No. NND2021085). The camels were owned by a local farm, and informed consent was obtained from the owner.

Consent for publication

Not applicable.

Funding

This work was supported by the Double First-Class Fund for Introducing Outstanding Doctoral Talents in Genomics and Biotechnology (Grant No. DC2000001589).

Authors' contributions

Yanru Zhang: Conceptualization, Methodology, Data curation, Writing – original draft.Yu Ling: Data analysis, Writing – review & editing.All authors have read and approved the final manuscript.

References

1. Krause M, Bock PM, Takahashi HK, Homem De Bittencourt PI, Jr., Newsholme P: The regulatory roles of NADPH oxidase, intra- and extra-cellular HSP70 in pancreatic islet function, dysfunction and diabetes. Clin Sci (Lond) 2015;128:789-803.
2. Mukherjee A, Morales-Scheihing D, Butler PC, Soto C: Type 2 diabetes as a protein misfolding disease. Trends Mol Med 2015;21:439-449.
3. Bagnati M, Ogunkolade BW, Marshall C, Tucci C, Hanna K, Jones TA, Bugliani M, Nedjai B, Caton PW, Kieswich J, Yaqoob MM, Ball GR, Marchetti P, Hitman GA, Turner MD: Glucolipotoxicity initiates pancreatic beta-cell death through TNFR5/CD40-mediated STAT1 and NF-kappaB activation. Cell Death Dis 2016;7:e2329.
4. Federici M, Hribal M, Perego L, Ranalli M, Caradonna Z, Perego C, Usellini L, Nano R, Bonini P, Bertuzzi F: High glucose causes apoptosis in cultured human pancreatic islets of Langerhans: a potential role for regulation of specific Bcl family genes toward an apoptotic cell death program. Diabetes 2001;50:1290.
5. Laybutt DR, Kaneto H, Hasenkamp W, Grey S, Jonas JC, Sgroi DC, Groff A, Ferran C, Bonner-Weir S, Sharma A: Increased expression of antioxidant and antiapoptotic genes in islets that may contribute to beta-cell survival during chronic hyperglycemia. Diabetes 2002;51:413.
6. Corbet GB, Hill JE: Mammal Species of the World: A Taxonomic and Geographic Reference by D. E. Wilson; D. M. Reeder. Mastozoología Neotropical 2006;13:290-293.
7. Groves C, Grubb P: Ungulate Taxonomy. Johns Hopkins Ebook 2011
8. Potts D: Bactrian Camels and Bactrian-Dromedary Hybrids. 2015
9. Roberts, Michael: Biology - A Functional Approach. Nelson, 1982.
10. Bactrian Camels Genome S, Analysis C, Jirimutu, Wang Z, Ding G, Chen G, Sun Y, Sun Z, Zhang H, Wang L, Hasi S, Zhang Y, Li J, Shi Y, Xu Z, He C, Yu S, Li S, Zhang W, Batmunkh M, Ts B, Narenbatu, Unierhu, Bat-Ireedui S, Gao H, Baysgalan B, Li Q, Jia Z, Turigenbayila, Subudenggerile, Narenmanduhu, Wang Z, Wang J, Pan L, Chen Y, Ganerdene Y, Dabxilt, Erdemt, Altansha, Altansukh, Liu T, Cao M, Aruuntsever, Bayart, Hosblig, He F, Zha-ti A, Zheng G, Qiu F, Sun Z, Zhao L, Zhao W, Liu B, Li C, Chen Y, Tang X, Guo C, Liu W, Ming L, Temuulen, Cui A, Li Y, Gao J, Li J, Wurentaodi, Niu S, Sun T, Zhai Z, Zhang M, Chen C, Baldan T, Bayaer T, Li Y, Meng H: Genome sequences of wild and domestic bactrian camels. Nat Commun 2012;3:1202.

11. Kaske M, Elmahdi B, Von EW, Sallmann HP: Insulin responsiveness of sheep, ponies, miniature pigs and camels: results of hyperinsulinemic clamps using porcine insulin. Journal of Comparative Physiology B Biochemical Systemic & Environmental Physiology 2001;171:549.
12. Elmahdi B, Sallmann HP, Fuhrmann H, Von EW, Kaske M: Comparative aspects of glucose tolerance in camels, sheep, and ponies. Comparative Biochemistry & Physiology Part A Physiology 1997;118:147.
13. American Diabetes A: Diagnosis and classification of diabetes mellitus. Diabetes Care 2010;33 Suppl 1:S62-69.
14. Medicine IOC: Definition and diagnosis of diabetes mellitus and intermediate hyperglycemia. Geneva World Health Organization 2006
15. DREAM: Effect of rosiglitazone on the frequency of diabetes in patients with impaired glucose tolerance or impaired fasting glucose: a randomised controlled trial. The Lancet 2006;368:1096-1105.
16. Wu H, Guang X, Al-Fageeh MB, Cao J, Pan S, Zhou H, Zhang L, Abutarboush MH, Xing Y, Xie Z, Alshanqeeti AS, Zhang Y, Yao Q, Al-Shomrani BM, Zhang D, Li J, Manee MM, Yang Z, Yang L, Liu Y, Zhang J, Altammami MA, Wang S, Yu L, Zhang W, Liu S, Ba L, Liu C, Yang X, Meng F, Wang S, Li L, Li E, Li X, Wu K, Zhang S, Wang J, Yin Y, Yang H, Al-Swailem AM, Wang J: Camelid genomes reveal evolution and adaptation to desert environments. Nat Commun 2014;5:5188.
17. Langmead B, Salzberg SL: Fast gapped-read alignment with Bowtie 2. Nature Methods 2012;9:357.
18. Trapnell C: TopHat2: accurate alignment of transcriptomes in the presence of insertions, deletions and gene fusions. Genome Biology 2013;14:R36.
19. Anders S, Pyl PT, Huber W: HTSeq—a Python framework to work with high-throughput sequencing data. Bioinformatics 2015;31:166-169.
20. Robinson MD, Mccarthy DJ, Smyth GK: edgeR: a Bioconductor package for differential expression analysis of digital gene expression data. Bioinformatics 2010;26:139-140.
21. Wang L, Feng Z, Wang X, Wang X, Zhang X: DEGseq: an R package for identifying differentially expressed genes from RNA-seq data. Bioinformatics 2010;26:136.
22. Perkins DN, Pappin DJ, Creasy DM, Cottrell JS: Probability-based protein identification by searching sequence databases using mass spectrometry data. Electrophoresis 1999;20:3551.
23. Vizcaino JA, Csordas A, del-Toro N, Dianes JA, Griss J, Lavidas I, Mayer G, Perez-Riverol Y, Reisinger F, Ternent T, Xu QW, Wang R, Hermjakob H: 2016 update of the PRIDE database and its related tools. Nucleic Acids Res 2016;44:D447-456.
24. Sleep D, Cameron J, Evans LR: Albumin as a versatile platform for drug half-life extension. Biochim Biophys Acta 2013;1830:5526-5534.
25. Rd TAB, Graham MJ, Baker BF, Crooke RM: Therapeutic inhibition of apoC-III for the treatment of hypertriglyceridemia. Clinical Lipidology 2015;10:191-203.

26. Hill KE, Wu S, Motley AK, Stevenson TD, Winfrey VP, Capecchi MR, Atkins JF, Burk RF: Production of selenoprotein P (Sepp1) by hepatocytes is central to selenium homeostasis. J Biol Chem 2012;287:40414-40424.
27. Hajarnis SS, Patel V, Aboudehen K, Attanasio M, Cobo-Stark P, Pontoglio M, Igarashi P: Transcription Factor Hepatocyte Nuclear Factor-1beta (HNF-1beta) Regulates MicroRNA-200 Expression through a Long Noncoding RNA. J Biol Chem 2015;290:24793-24805.
28. Kuma A, Tamura M, Ishimatsu N, Miyamoto T, Serino R, Ishimori S, Morisada N, Iijima K, Yamada S, Takeuchi M, Abe H, Otsuji Y: A novel UMOD gene mutation associated with uromodulin-associated kidney disease in a young woman with moderate kidney dysfunction. Intern Med 2015;54:631-635.
29. Richter GW: A study of hemosiderosis with the aid of electron microscopy. With observations on the relationship between hemosideriu and ferritin. Journal of Experimental Medicine 1957;106:203.
30. Chang Y, Wang SX, Wang YB, Zhou J, Li WH, Wang N, Fang DF, Li HY, Li AL, Zhang XM, Zhang WN: ECHS1 interacts with STAT3 and negatively regulates STAT3 signaling. FEBS Lett 2013;587:607-613.
31. Dvergsten J, Manivel JC, Correa-Rotter R, Rosenberg ME: Expression of clusterin in human renal diseases. Kidney International 1994;45:828-835.
32. Masson E, Chen JM, Audrezet MP, Cooper DN, Ferec C: A conservative assessment of the major genetic causes of idiopathic chronic pancreatitis: data from a comprehensive analysis of PRSS1, SPINK1, CTRC and CFTR genes in 253 young French patients. PLoS One 2013;8:e73522.
33. Marchegiani G, Paulo JA, Sahora K, Fernandez-Del Castillo C: The proteome of postsurgical pancreatic juice. Pancreas 2015;44:574-582.
34. Michael Carrion JC: Identification of Differentially Expressed Genes in Pancreatic Regulatory T-Cell Survivalc. Journal of Diabetes & Metabolism 2015;6
35. Fjeld K, Weiss FU, Lasher D, Rosendahl J, Chen JM, Johansson BB, Kirsten H, Ruffert C, Masson E, Steine SJ, Bugert P, Cnop M, Grutzmann R, Mayerle J, Mossner J, Ringdal M, Schulz HU, Sendler M, Simon P, Sztromwasser P, Torsvik J, Scholz M, Tjora E, Ferec C, Witt H, Lerch MM, Njolstad PR, Johansson S, Molven A: A recombined allele of the lipase gene CEL and its pseudogene CELP confers susceptibility to chronic pancreatitis. Nat Genet 2015;47:518-522.
36. Fjeld K, Beer S, Johnstone M, Zimmer C, Mossner J, Ruffert C, Krehan M, Zapf C, Njolstad PR, Johansson S, Bugert P, Miyajima F, Liloglou T, Brown LJ, Winn SA, Davies K, Latawiec D, Gunson BK, Criddle DN, Pirmohamed M, Grutzmann R, Michl P, Greenhalf W, Molven A, Sutton R, Rosendahl J: Length of Variable Numbers of Tandem Repeats in the Carboxyl Ester Lipase (CEL) Gene May Confer Susceptibility to Alcoholic Liver Cirrhosis but Not Alcoholic Chronic Pancreatitis. PLoS One 2016;11:e0165567.
37. Rasanen K, Lehtinen E, Nokelainen K, Kuopio T, Hautala L, Itkonen O, Stenman UH, Koistinen H: Interleukin-6 increases expression of serine protease inhibitor Kazal type 1 through STAT3 in colorectal adenocarcinoma. Mol Carcinog 2016;55:2010-2023.
38. Pirozhkova I, Barat A, Dmitriev P, Kim E, Robert T, Guegan J, Bilhou-Nabera C, Busato F, Tost J, Carnac G, Laoudj-Chenivesse D, Lipinski M, Vassetzky Y: Differences in transcription patterns

between induced pluripotent stem cells produced from the same germ layer are erased upon differentiation. PLoS One 2013;8:e53033.

39. Zhao Y, Li J, Liu H, Xi Y, Xue M, Liu W, Zhuang Z, Lei M: Dynamic transcriptome profiles of skeletal muscle tissue across 11 developmental stages for both Tongcheng and Yorkshire pigs. BMC Genomics 2015;16:377.
40. Holt I, Duong NT, Zhang Q, Lam le T, Sewry CA, Mamchaoui K, Shanahan CM, Morris GE: Specific localization of nesprin-1-alpha2, the short isoform of nesprin-1 with a KASH domain, in developing, fetal and regenerating muscle, using a new monoclonal antibody. BMC Cell Biol 2016;17:26.
41. Haolin C: Cloning, structural analysis and expression of cardiac troponin C (TNNC1) gene in goat. African Journal of Biotechnology 2012;11
42. Nyasavajjala SM, Phillips BE, Lund JN, Williams JP: Creatinine and myoglobin are poor predictors of anaerobic threshold in colorectal cancer and health. J Cachexia Sarcopenia Muscle 2015;6:125-131.
43. Fujita M, Mitsuhashi H, Isogai S, Nakata T, Kawakami A, Nonaka I, Noguchi S, Hayashi YK, Nishino I, Kudo A: Filamin C plays an essential role in the maintenance of the structural integrity of cardiac and skeletal muscles, revealed by the medaka mutant zacro. Dev Biol 2012;361:79-89.
44. Joureau B, de Winter JM, Pappas CT, Malfatti E, Beggs A, Clarke N, Romero N, Gregorio C, Granzier H, Stienen GJM, Ottenheijm CCA: Force-Sarcomere Length Relations in Patients with Thin Filament Myopathy Caused by Mutations in NEB, ACTA1, TPM2, TPM3, KBTBD13, KLHL40 and KLHL41. Biophysical Journal 2015;108:338a-339a.
45. Roman M, Jitaru P, Barbante C: Selenium biochemistry and its role for human health. Metallomics 2014;6:25-54.
46. Nahomi RB, DiMauro MA, Wang B, Nagaraj RH: Identification of peptides in human Hsp20 and Hsp27 that possess molecular chaperone and anti-apoptotic activities. Biochem J 2015;465:115-125.
47. Chow AM, Mok P, Xiao D, Khalouei S, Brown IR: Heteromeric complexes of heat shock protein 70 (HSP70) family members, including Hsp70B', in differentiated human neuronal cells. Cell Stress Chaperones 2010;15:545-553.
48. Khalouei S, Chow AM, Brown IR: Stress-induced localization of HSPA6 (HSP70B') and HSPA1A (HSP70-1) proteins to centrioles in human neuronal cells. Cell Stress Chaperones 2014;19:321-327.
49. Yi J, Yun J, Li ZK, Xu CT, Pan BR: Epidemiology and molecular genetics of congenital cataracts. Int J Ophthalmol 2011;4:422-432.
50. Xie J, Dai C, Hu X: Evidence That Does Not Support Pyruvate Kinase M2 (PKM2)-catalyzed Reaction as a Rate-limiting Step in Cancer Cell Glycolysis. J Biol Chem 2016;291:8987-8999.
51. Wilson JE: Isozymes of mammalian hexokinase: structure, subcellular localization and metabolic function. Journal of Experimental Biology 2003;206:2049-2057.
52. Hayward BE, Fantes JA, Warner JP, Intody S, Leek JP, Markham AF, Bonthron DT: Co-localization of the ketohexokinase and glucokinase regulator genes to a 500-kb region of Chromosome 2p23.

Mammalian Genome Official Journal of the International Mammalian Genome Society 1996;7:454-458.

53. Wang ZY, Jin L, Tan H, Irwin DM: Evolution of hepatic glucose metabolism: liver-specific glucokinase deficiency explained by parallel loss of the gene for glucokinase regulatory protein (GCKR). PLoS One 2013;8:e60896.
54. Melis D, Fulceri R, Parenti G, Marcolongo P, Gatti R, Parini R, Riva E, Della Casa R, Zammarchi E, Andria G, Benedetti A: Genotype/phenotype correlation in glycogen storage disease type 1b: a multicentre study and review of the literature. Eur J Pediatr 2005;164:501-508.
55. Mankowski RT, Anton SD, Buford TW, Leeuwenburgh C: Dietary Antioxidants as Modifiers of Physiologic Adaptations to Exercise. Med Sci Sports Exerc 2015;47:1857-1868.
56. Ai PHL, Hua H, Chuong PH: Free Radicals, Antioxidants in Disease and Health. International Journal of Biomedical Science Ijbs 2008;4:89-96.
57. Zelko IN, Mariani TJ, Folz RJ: Superoxide dismutase multigene family: a comparison of the CuZn-SOD (SOD1), Mn-SOD (SOD2), and EC-SOD (SOD3) gene structures, evolution, and expression. Free Radical Biology & Medicine 2002;33:337-349.
58. Robertson RP: Chronic oxidative stress as a central mechanism for glucose toxicity in pancreatic islet beta cells in diabetes. J Biol Chem 2004;279:42351-42354.
59. Newsholme P, Haber EP, Hirabara SM, Rebelato EL, Procopio J, Morgan D, Oliveira-Emilio HC, Carpinelli AR, Curi R: Diabetes associated cell stress and dysfunction: role of mitochondrial and non-mitochondrial ROS production and activity. J Physiol 2007;583:9-24.
60. Venner TJ, Singh B, Gupta RS: Nucleotide sequences and novel structural features of human and Chinese hamster hsp60 (chaperonin) gene families. Dna & Cell Biology 1990;9:545-552.
61. Kregel KC: Heat shock proteins: modifying factors in physiological stress responses and acquired thermotolerance. Journal of Applied Physiology 2002;92:2177.
62. Wright EM, Turk E: The sodium/glucose cotransport family SLC5. Pflugers Arch 2004;447:510-518.
63. W. Waring S, J. Webb D, R. J. Maxwell S: Systemic Uric Acid Administration Increases Serum Antioxidant Capacity in Healthy Volunteers. Journal of Cardiovascular Pharmacology 2001;38:365-371.
64. Mandal AK, Mount DB: The molecular physiology of uric acid homeostasis. Annu Rev Physiol 2015;77:323-345.
65. Brouwers MC, Jacobs C, Bast A, Stehouwer CD, Schaper NC: Modulation of Glucokinase Regulatory Protein: A Double-Edged Sword? Trends Mol Med 2015;21:583-594.
66. Schaftingen EV, Vandercammen A, Detheux M, Davies DR: The regulatory protein of liver glucokinase. Advances in Enzyme Regulation 1992;32:133-148.
67. Iynedjian PB, Pilot PR, Nouspikel T, Milburn JL, Quaade C, Hughes S, Ucla C, Newgard CB: Differential expression and regulation of the glucokinase gene in liver and islets of Langerhans. P Natl Acad Sci USA 1989;86:7838.

68. Vallon V, Platt KA, Cunard R, Schroth J, Whaley J, Thomson SC, Koepsell H, Rieg T: SGLT2 mediates glucose reabsorption in the early proximal tubule. J Am Soc Nephrol 2011;22:104-112.
69. Bonner C, Kerr-Conte J, Gmyr V, Queniat G, Moerman E, Thevenet J, Beaucamps C, Delalleau N, Popescu I, Malaisse WJ, Sener A, Deprez B, Abderrahmani A, Staels B, Pattou F: Inhibition of the glucose transporter SGLT2 with dapagliflozin in pancreatic alpha cells triggers glucagon secretion. Nat Med 2015;21:512-517.
70. Pei L, Waki H, Vaitheesvaran B, Wilpitz DC, Kurland IJ, Tontonoz P: NR4A orphan nuclear receptors are transcriptional regulators of hepatic glucose metabolism. Nat Med 2006;12:1048-1055.
71. Gerich JE: Role of the kidney in normal glucose homeostasis and in the hyperglycaemia of diabetes mellitus: therapeutic implications. Diabet Med 2010;27:136-142.
72. Karas M, Hillenkamp F: Laser desorption ionization of proteins with molecular masses exceeding 10,000 daltons. Analytical Chemistry 1988;60:2299.
73. Alshahrani S, Almutairi MM, Kursan S, Dias-Junior E, Almiahuob MM, Aguilar-Bryan L, Di Fulvio M: Increased Slc12a1 expression in beta-cells and improved glucose disposal in Slc12a2 heterozygous mice. J Endocrinol 2015;227:153-165.
74. Soty M, Chilloux J, Casteras S, Grichine A, Mithieux G, Gautier-Stein A: New insights into the organisation and intracellular localisation of the two subunits of glucose-6-phosphatase. Biochimie 2012;94:695.
75. Maritim AC, Sanders RA, Watkins JB: Effects of α-lipoic acid on biomarkers of oxidative stress in streptozotocin-induced diabetic rats. The Journal of Nutritional Biochemistry 2003;14:288-294.
76. Nishikawa M, Hashida M, Takakura Y: Catalase delivery for inhibiting ROS-mediated tissue injury and tumor metastasis. Advanced Drug Delivery Reviews 2009;61:319-326.
77. Prabhakar R, Vreven T, Morokuma K, Musaev DG: Elucidation of the mechanism of selenoprotein glutathione peroxidase (GPx)-catalyzed hydrogen peroxide reduction by two glutathione molecules: a density functional study. Biochemistry 2005;44:11864-11871.
78. Ceriello A, Dello RP, Amstad P, Cerutti P: High glucose induces antioxidant enzymes in human endothelial cells in culture. Evidence linking hyperglycemia and oxidative stress. Diabetes 1996;45:471-477.
79. Abu-Farha M, Cherian P, Al-Khairi I, Tiss A, Khadir A, Kavalakatt S, Warsame S, Dehbi M, Behbehani K, Abubaker J: DNAJB3/HSP-40 cochaperone improves insulin signaling and enhances glucose uptake in vitro through JNK repression. Sci Rep 2015;5:14448.
80. Nollen EA, Morimoto RI: Chaperoning signaling pathways: molecular chaperones as stress-sensing 'heat shock' proteins. Journal of Cell Science 2002;115:2809.
81. Motiei M, Tavalaee M, Rabiei F, Hajihosseini R, Nasr-Esfahani MH: Evaluation of HSPA2 in fertile and infertile individuals. Andrologia 2013;45:66-72.
82. James P, Pfund C, Craig EA: Functional Specificity Among Hsp70 Molecular Chaperones. Science 1997;275:387.

83. Wan Y, Ma C, Wei P, Fang Q, Guo X, Zhou B, Jiang R: Dynamic expression of HSP90B1 mRNA in the hypothalamus of two Chinese chicken breeds under heat stress and association analysis with a SNP in Huainan chickens. Czech Journal of Animal Science 2017;62:82-87.
84. Zuehlke AD, Beebe K, Neckers L, Prince T: Regulation and function of the human HSP90AA1 gene. Gene 2015;570:8-16.
85. Qi W, Chen X, Gilbert RE, Zhang Y, Waltham M, Schache M, Kelly DJ, Pollock CA: High glucose-induced thioredoxin-interacting protein in renal proximal tubule cells is independent of transforming growth factor-beta1. Am J Pathol 2007;171:744-754.
86. Cheng MY, Hartl FU, Martin J, Pollock RA, Kalousek F, Neupert W, Hallberg EM, Hallberg RL, Horwich AL: Mitochondrial heat-shock protein hsp60 is essential for assembly of proteins imported into yeast mitochondria. Nature 1989;337:620.
87. Ostermann J, Horwich AL, Neupert W, Hartl FU: Protein folding in mitochondria requires complex formation with hsp60 and ATP hydrolysis. Nature 1989;341:125-130.
88. Sullivan MA, Olson CL, Winquist AG, Engman DM: EXPRESSION AND LOCALIZATION OF TRYPANOSOMA CRUZI HSP60. Molecular and Biochemical Parasitology 1994;68:197-208.
89. Martin J, Horwich AL, Hartl FU: Prevention of protein denaturation under heat stress by the chaperonin Hsp60. Science 1992;258:995.
90. Cajo GC, Horne BE, Kelley WL, Schwager F, Georgopoulos C, Genevaux P: The role of the DIF motif of the DnaJ (Hsp40) co-chaperone in the regulation of the DnaK (Hsp70) chaperone cycle. J Biol Chem 2006;281:12436-12444.
91. Michels AA, Kanon B, Konings AW, Ohtsuka K, Bensaude O, Kampinga HH: Hsp70 and Hsp40 chaperone activities in the cytoplasm and the nucleus of mammalian cells. Journal of Biological Chemistry 1997;272:33283-33289.
92. Jacquier-Sarlin MR, Fuller K, Dinh-Xuan AT, Richard MJ, Polla BS: protective effect f HSP70 in inflammation. 1994.
93. Barteltkirbach B, Golenhofen N: Erratum to: Reaction of small heat-shock proteins to different kinds of cellular stress in cultured rat hippocampal neurons. Cell Stress & Chaperones 2014;19:145-153.
94. Schwarz L, Vollmer G, Richter-Landsberg C: The Small Heat Shock Protein HSP25/27 (HspB1) Is Abundant in Cultured Astrocytes and Associated with Astrocytic Pathology in Progressive Supranuclear Palsy and Corticobasal Degeneration. Int J Cell Biol 2010;2010:717520.
95. Préville X, Salvemini F, Giraud S, Chaufour S, Paul C, Stepien G, Ursini MV, Arrigo AP: Mammalian Small Stress Proteins Protect against Oxidative Stress through Their Ability to Increase Glucose-6-phosphate Dehydrogenase Activity and by Maintaining Optimal Cellular Detoxifying Machinery . Experimental Cell Research 1999;247:61-78.
96. Sanchez-Nino MD, Sanz AB, Sanchez-Lopez E, Ruiz-Ortega M, Benito-Martin A, Saleem MA, Mathieson PW, Mezzano S, Egido J, Ortiz A: HSP27/HSPB1 as an adaptive podocyte antiapoptotic protein activated by high glucose and angiotensin II. Lab Invest 2012;92:32-45.

97. Ramirez VP, Stamatis M, Shmukler A, Aneskievich BJ: Basal and stress-inducible expression of HSPA6 in human keratinocytes is regulated by negative and positive promoter regions. Cell Stress Chaperones 2015;20:95-107.
98. Liu L, Qi X, Chen Z, Shaw L, Cai J, Smith LH, Grant MB, Boulton ME: Targeting the IRE1alpha/XBP1 and ATF6 arms of the unfolded protein response enhances VEGF blockade to prevent retinal and choroidal neovascularization. Am J Pathol 2013;182:1412-1424.
99. Ghosh JG, Jr SA, Clark JI: Interactions between important regulatory proteins and human alphaB crystallin. Biochemistry 2007;46:6308.
100. Singhal M, Rasania S, Gaur A, Vishnu VRM, Vijaya S, Raju R, Upadhyay Y: Overview on Sodium Glucose Transport Inhibitors as a Therapeutic Tool Against Diabetes Mellitus. 2012;6
101. Wright EM: Glucose transport families SLC5 and SLC50. Mol Aspects Med 2013;34:183-196.
102. Glantzounis GK, Tsimoyiannis EC, Kappas AM, Galaris DA: Uric acid and oxidative stress. Current Pharmaceutical Design 2005;11:-.
103. Ames BN, Cathcart R, Schwiers E, Hochstein P: Uric acid provides an antioxidant defense in humans against oxidant- and radical-caused aging and cancer: a hypothesis. P Natl Acad Sci USA 1981;78:6858.
104. Amaro S, Llull L, Renu A, Laredo C, Perez B, Vila E, Torres F, Planas AM, Chamorro A: Uric acid improves glucose-driven oxidative stress in human ischemic stroke. Ann Neurol 2015;77:775-783.
105. Burk RF, Olson GE, Winfrey VP, Hill KE, Yin D: Glutathione peroxidase-3 produced by the kidney binds to a population of basement membranes in the gastrointestinal tract and in other tissues. Am J Physiol Gastrointest Liver Physiol 2011;301:G32-38.
106. Iida R, Tsubota E, Takeshita H, Yasuda T: Multiplex single base extension method for simultaneous genotyping of non-synonymous SNP in the three human SOD genes. Electrophoresis 2008;29:4788-4794.
107. Folz RJ, Guan J, Seldin MF, Oury TD, Enghild JJ, Crapo JD: Mouse Extracellular Superoxide Dismutase: Primary Structure, Tissue-specific Gene Expression, Chromosomal Localization, and Lung In Situ Hybridization. American Journal of Respiratory Cell & Molecular Biology 1997;17:393.
108. Fujita H, Fujishima H, Chida S, Takahashi K, Qi Z, Kanetsuna Y, Breyer MD, Harris RC, Yamada Y, Takahashi T: Reduction of renal superoxide dismutase in progressive diabetic nephropathy. J Am Soc Nephrol 2009;20:1303-1313.
109. Tiwari BK, Pandey KB, Abidi AB, Rizvi SI: Markers of Oxidative Stress during Diabetes Mellitus. J Biomark 2013;2013:378790.
110. Iwata K, Nishinaka T, Matsuno K, Yabe NC: Increased gene expression of glutathione peroxidase-3 in diabetic mouse heart. Biological & Pharmaceutical Bulletin 2006;29:1042-1045.
111. Folz RJ, Crapo JD: Extracellular superoxide dismutase (SOD3): tissue-specific expression, genomic characterization, and computer-assisted sequence analysis of the human EC SOD gene. Genomics 1994;22:162-171.

Figures

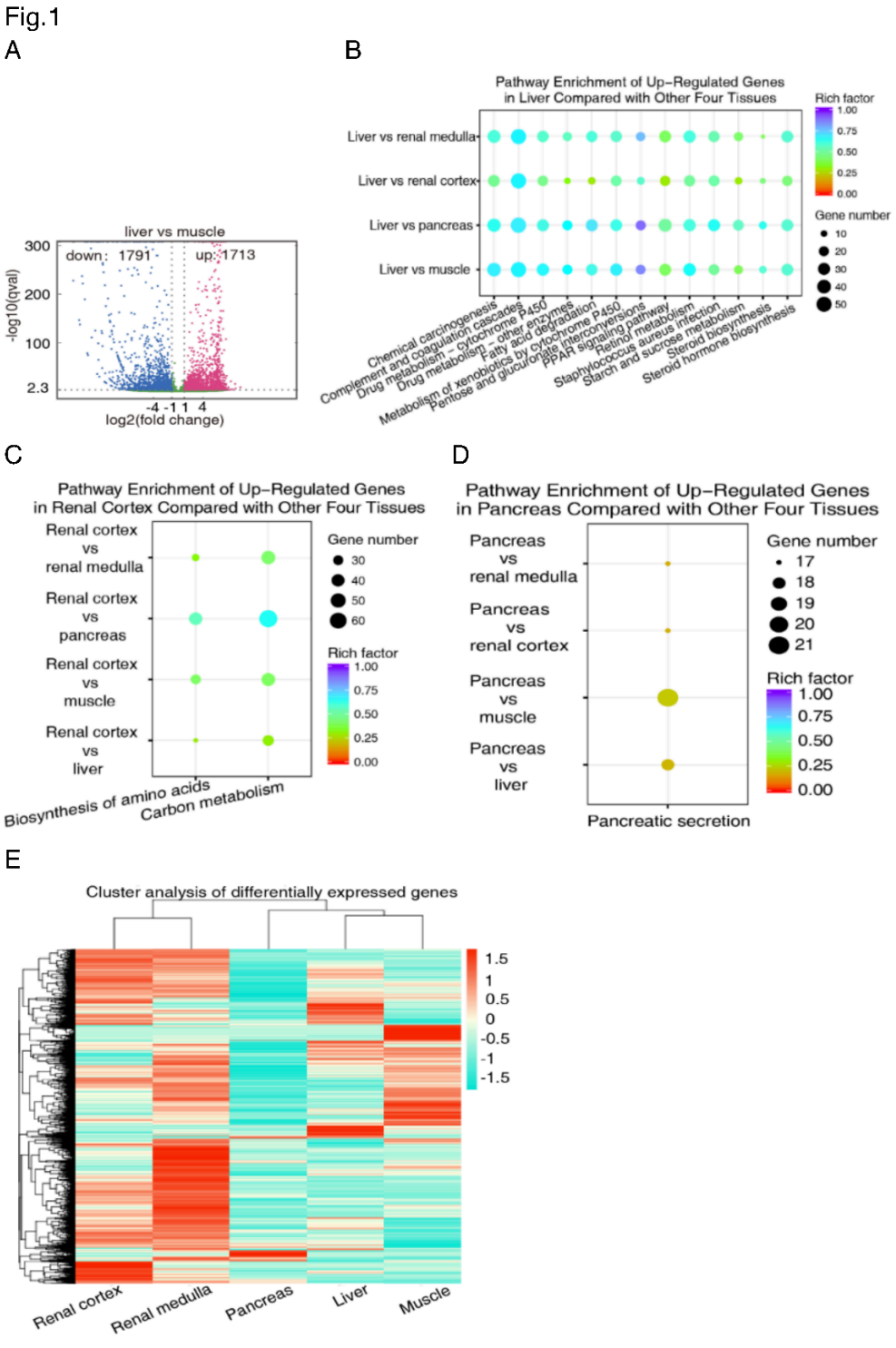


Figure 1

Camels' liver, Pancreas, Renal Cortex, Renal Medulla, and Muscle Functional Characteristics and Gene Expression Differences

Liver, pancreas, muscle, renal medulla, and renal cortex were obtained from the normal camels living in the natural environment. Tissues were isolated, and RNA was extracted for RNA-sequencing. Differentially expressed genes between the tissues were obtained by DEGSeq and TMM.

(A) Log2 fold changes in exons of RefSeq gene bodies in two tissues were employed and the corresponding significance values were displayed as -log10 (q-value). The red, blue and green dots indicate up-regulated, down-regulated and no significant difference genes, respectively (the threshold of differential expression: |log2 (Fold Change)| > 1 & q-value < 0.005). The numbers represent the number of up-regulated and down-regulated genes in both tissues.

(B-D) All genes that were up-regulated in a tissue compared with the other four tissues were subjected to functional enrichment analyses using KOBAS (2.0). Significantly enriched (q-value < 0.05) metabolic pathways are extracted from the KEGG database, which were based on the up-regulated genes in a tissue relative to other four tissues. The vertical axis represents tissues, and the horizontal axis represents the enriched pathway. The size of the dots indicates the number of differentially expressed genes in the pathway, and the color of the point corresponds to the degree of enrichment (rich factor).

(E) The differentially expressed genes FPKM values of the five tissues were used to hierarchical clustering analysis which was performed to determine the expression patterns in each tissue. The overall FPKM hierarchical clustering map was clustered with log10 (FPKM + 1) values, and the red was for high expression genes and the blue for low expression genes.

Fig.2

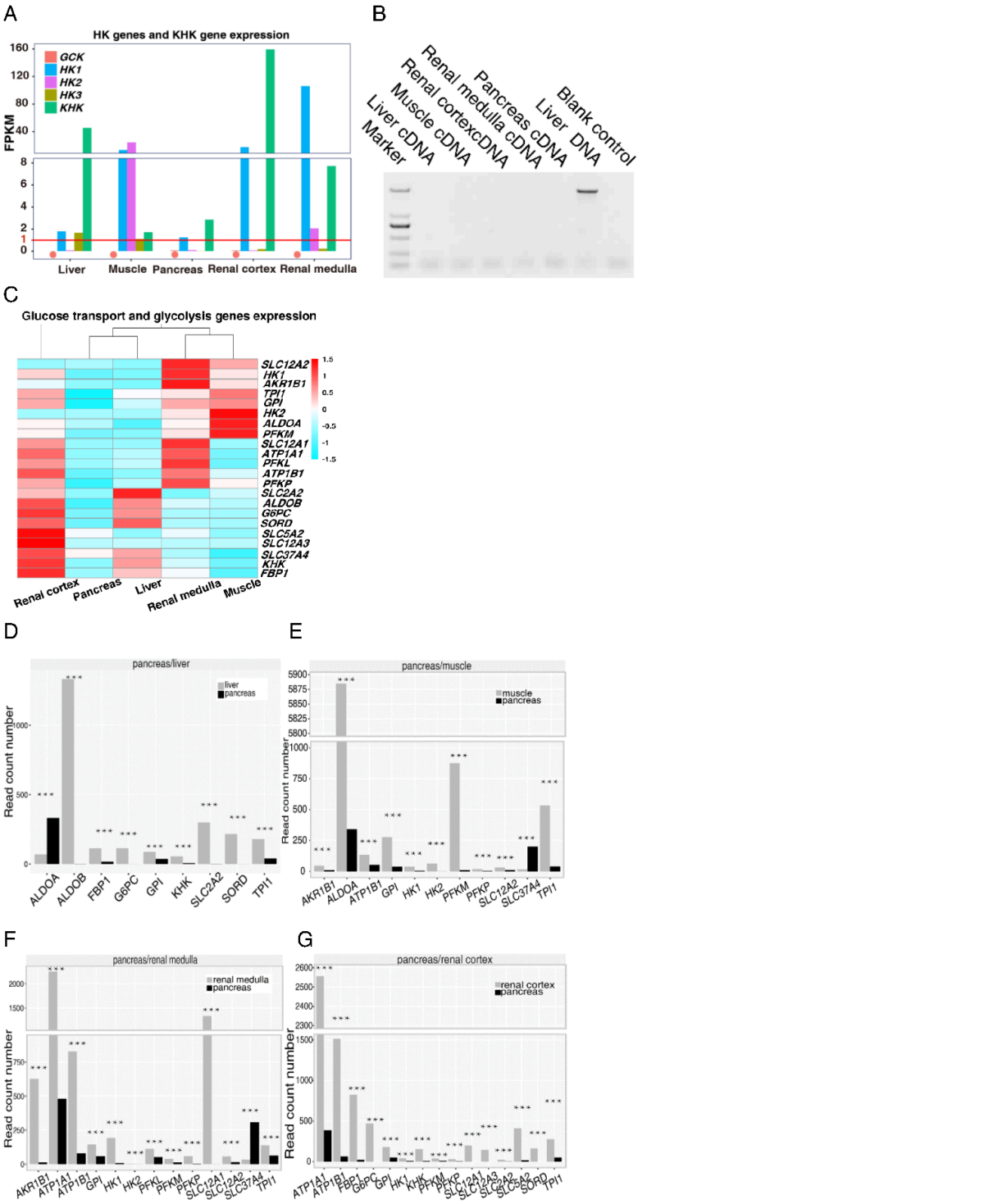


Figure 2

Expression of Glycolytic Genes in the Five Tissues

Read count number is Standardized.

(A) Relative expression levels of glycolytic rate-limiting enzyme genes and KHK gene from the RNA-seq dataset in the five tissues. The red line indicates the threshold of gene expression (FPKM = 1). FPKM > 1 means gene expression.

(B) Induction of *GCK* mRNA was measured by PCR in the five tissues, taking liver cDNA as the test group, liver DNA as the positive control group and water as the blank control group.

(C) Scaled expression values for the five tissues with all identified genes in glucose metabolism pathways (HK & KHK pathway and auxiliary transport route). The FPKM expression values for each sample were centered and scaled in the row direction (-1.5 - 1.5). Hierarchical clustering of samples was based on Pearson's correlation coefficient.

(D-G) Expression of the glycolytic pathway genes in pancreas *v.s*. the other four tissues. The thresholds of differential expression: |log2 (Fold Change)| > 1 & q-value < 0.005). Significance level: *** q-value < 0.001.

Fig.3

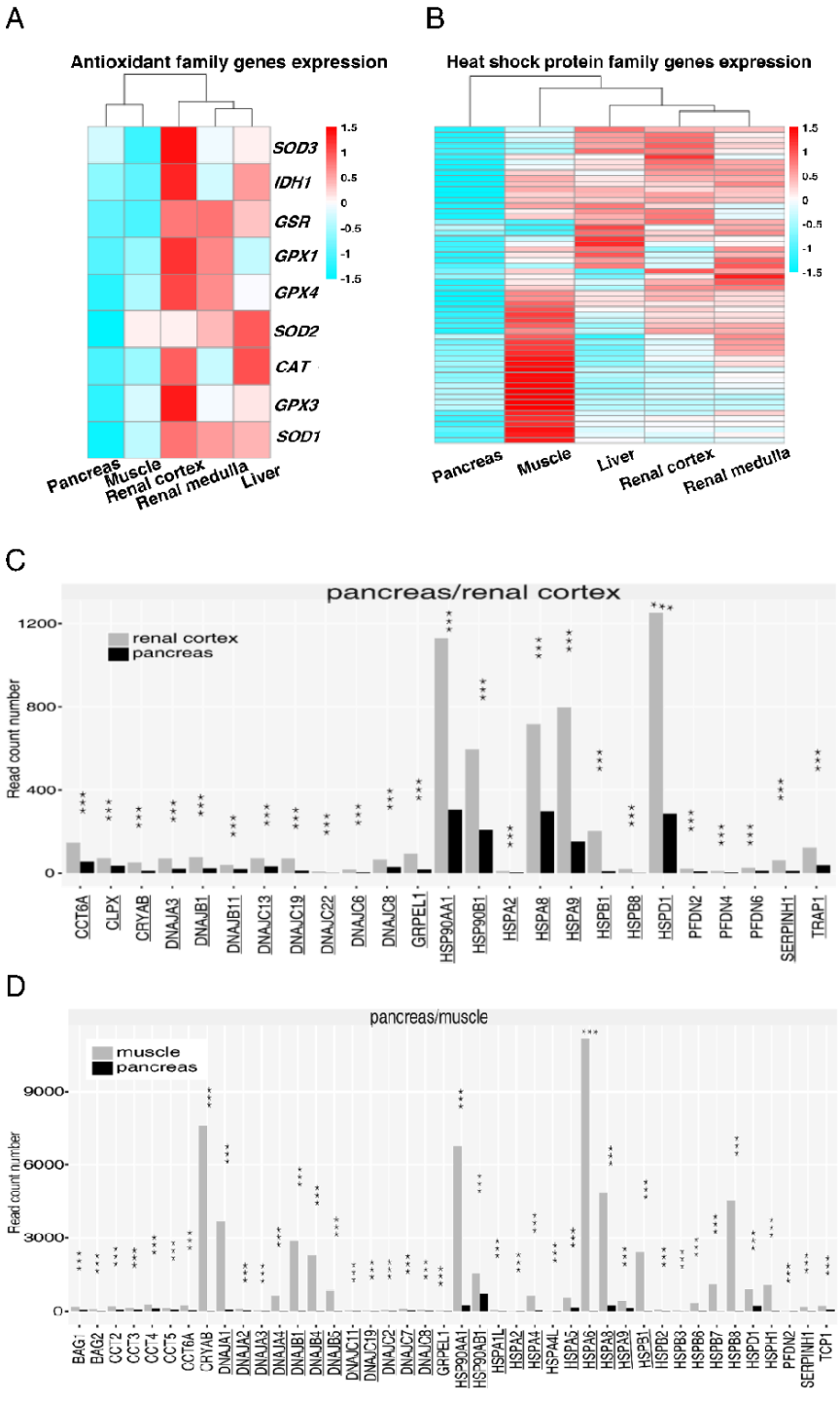


Figure 3

Expression Differences of HSP Family Genes and Antioxidant Genes in the Pancreas Compared with the Other Tissues

(A-B) Scaled expression values for the five tissues with all the identified genes in (A)antioxidant family and (B)heat shock protein family. The FPKM expression values for each sample were centered and

scaled in the row direction (-1.5–1.5). Hierarchical clustering of samples was based on Pearson's correlation coefficient.

(C-D) HSP family genes expression in pancreas *v.s.* renal cortex and pancreas *v.s.* muscle. The thresholds of differential expression: |log2 (Fold Change)| > 1 & q-value < 0.005). Significance level: *** q-value < 0.001.

Fig.4

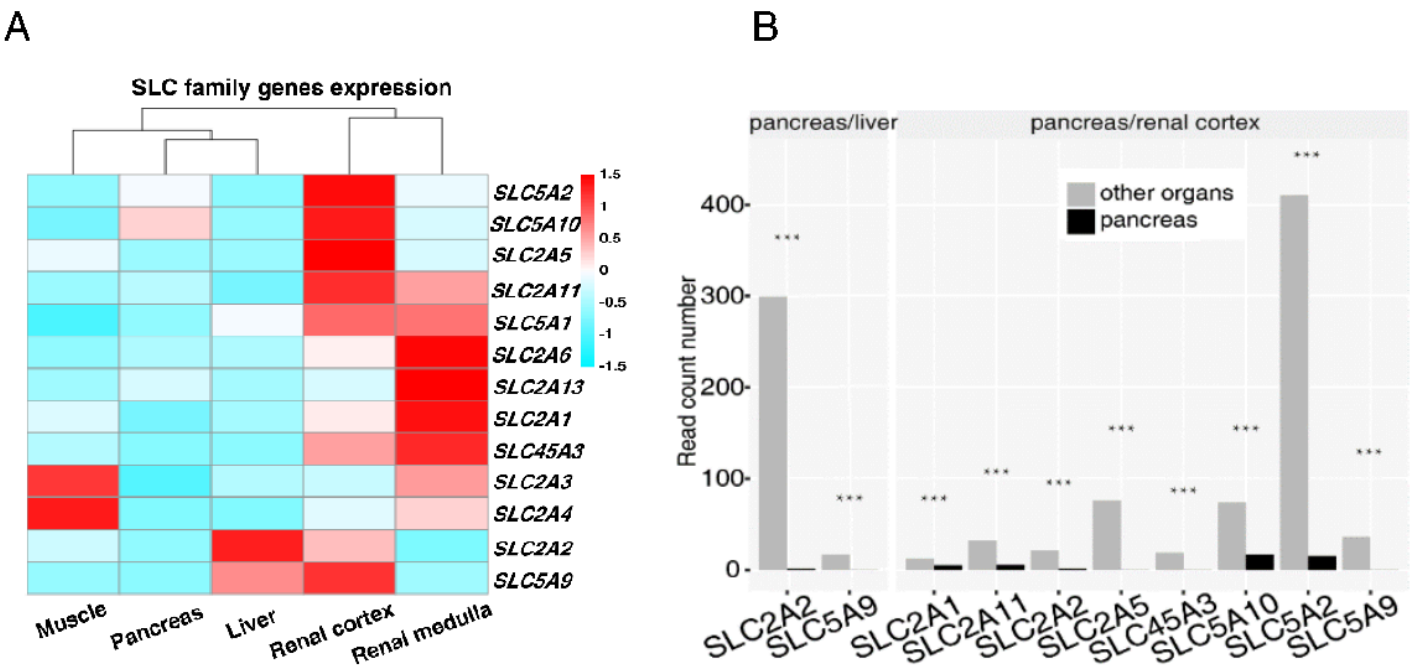


Figure 4

Genes Expression Differences of SLC Family in the Pancreas Compared with the Other Tissues

(A) Scaled expression values for the five tissues with all the identified genes in SLC family. The FPKM expression values for each sample were centered and scaled in the row direction (-1.5-1.5). Hierarchical clustering of samples was based on Pearson's correlation coefficient.

(B) HSP family genes expression in pancreas v.s. liver and pancreas v.s. renal cortex. The thresholds of differential expression: |log2 (Fold Change)| > 1 & q-value < 0.005). Significance level: *** q-value < 0.001.

Fig.5

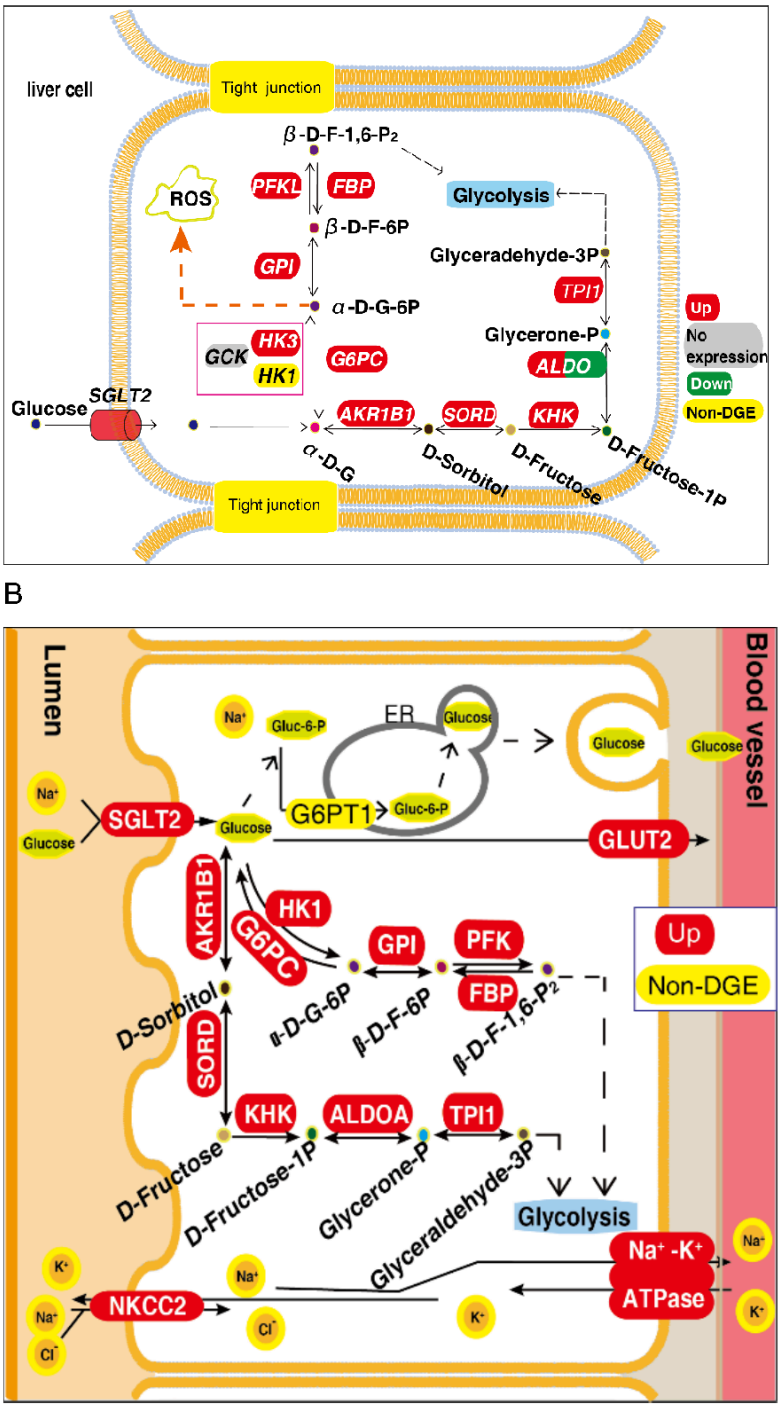


Figure 5

Glucose Metabolism and Transport are Active in Hepatocytes and Renal Cortical Cells

(A) Selected fructose and mannose metabolism (00051) and glycolysis pathway (00010) from KEGG, with indications of quantified genes (rectangles), are significantly regulated in renal cortex compared with pancreas under natural conditions. Colors indicate up-regulated (red), down-regulated (green), non-

expressed (yellow) and unexpressed (gray) expression levels of genes (encoding proteins that catalyze the indicated conversions) in renal cortex compared with pancreas under natural conditions. *AKRIB1*, aldo-keto reductase family 1 member B; *SORD*, sorbitol dehydrogenase; *KHK*, ketohexokinase; *ALDO*, aldolase, fructose-bisphosphate; *TPI1*, triosephosphate isomerase 1; *G6PC*, glucose-6-phosphatase; HXKI,hexokinase 1; *GPI*, glucose-6-phosphate isomerase; *PFKL*, phosphofructokinase, liver; *FBP*, fructose-1,6-bisphosphatase; *SGLT2*, sodium/glucose cotransporter 2; Glycolysis, Glycolysis pathway; ROS, reactive oxygen species; Gluc-6-P, D-Glucose 6-phosphate; D-Fructose-1P, D-Fructose 1-phosphate; Glycerone-P, D-Fructose 1-phosphate; Glyceradehyde-3P, Glyceraldehyde 3-phosphate; α-D-G-6P, alpha-D-Glucose 6-phosphate;β-D-F-6P, beta-D-Fructose 6-phosphate; β-D-F-1,6-P2, beta-D-Fructose 1,6-bisphosphate; *GCK*, glucokinase.

(B) Selected carbohydrate digestion and absorption (04973), fructose and mannose metabolism (00051) and glycolysis pathway (00010) from KEGG, with indications of quantified genes (rectangles), are significantly regulated in renal cortex compared with pancreas under natural conditions. Colors indicate increased (red), decreased (green), and unexpressed (gray) expression levels of genes (encoding proteins that catalyze the indicated conversions) in renal cortex compared with pancreas under natural conditions. AKRIB1, aldo-keto reductase family 1 member B; SORD, sorbitol dehydrogenase; KHK, ketohexokinase; ALDOA, aldolase, fructose-bisphosphate A; TPI1, triosephosphate isomerase 1; G6PC, glucose-6-phosphatase; HXKI,hexokinase 1; GPI, glucose-6-phosphate isomerase; PFKL, phosphofructokinase,liver; FBP, fructose-1,6-bisphosphatase; G6PT1, solute carrier family 37 member 4; GLUT2, solute carrier family 2 member 2; Na+ -K+ ATPase, ATPase Na+/K+ transporting subunit beta 1;NKCC2, Na-K-2Cl^- cotransporter; SGLT2, sodium/glucose cotransporter 2; Glycolysis, Glycolysis pathway; ROS, reactive oxygen species; ER, endoplasmic reticulum; Gluc-6-P, D-Glucose 6-phosphate; D-Fructose-1P, D-Fructose 1-phosphate; Glycerone-P, D-Fructose 1-phosphate; Glyceradehyde-3P, Glyceraldehyde 3-phosphate; α-D-G-6P, alpha-D-Glucose 6-phosphate;β-D-F-6P, beta-D-Fructose 6-phosphate; β-D-F-1,6-P2, beta-D-Fructose 1,6-bisphosphate.

Fig.6

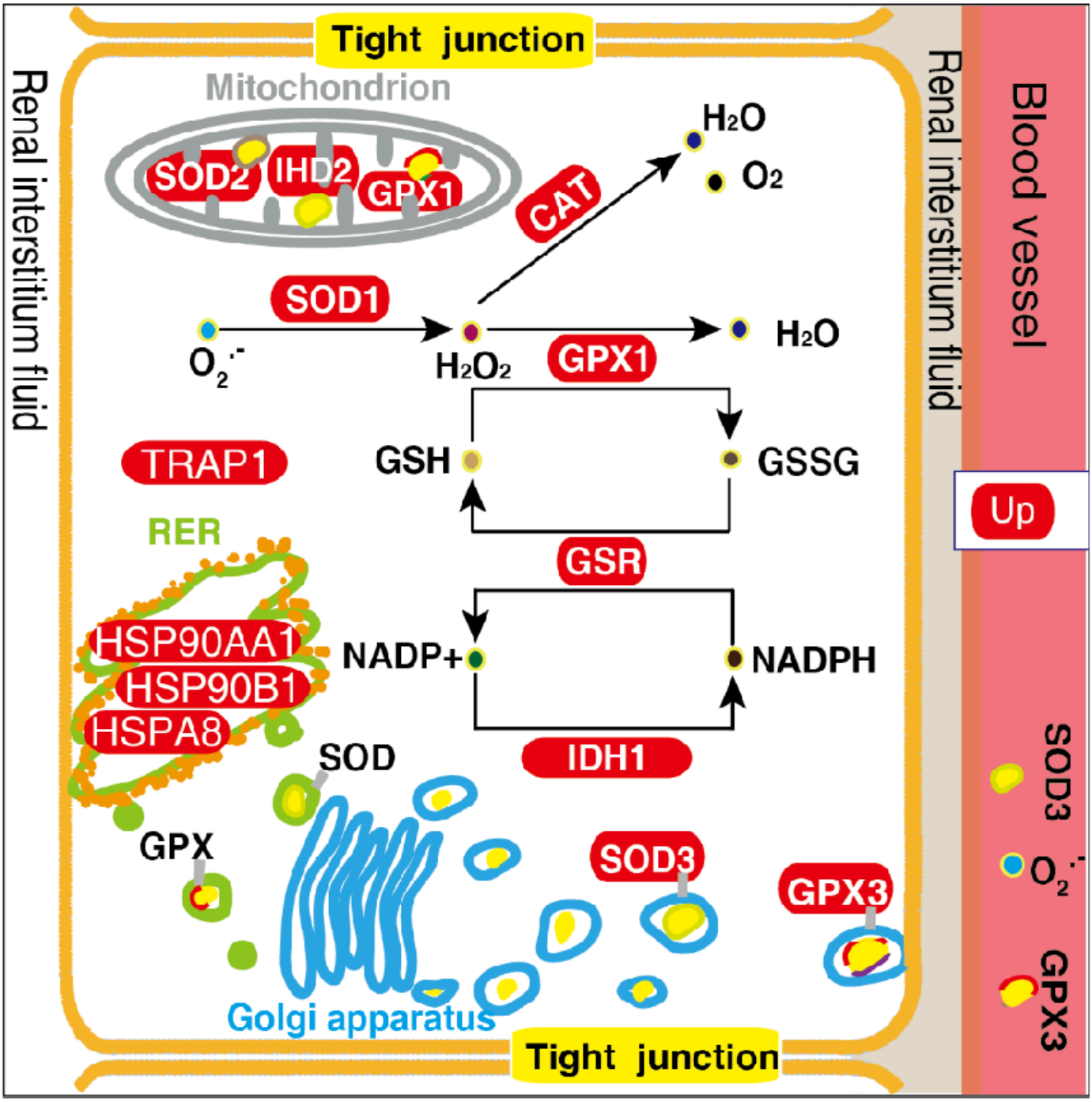


Figure 6

The Active Metabolism of Antioxidant Enzyme and HSP in the Renal Cortex Improves Environment of Cytoplasm, Endoplasmic Reticulum and Blood Vessel

Selected glutathione metabolism (00480) from KEGG, with indications of quantified genes (rectangles), is regulated significantly in renal cortex compared to pancreas and proteins corresponding to the genes

in renal cortex by PMS. Red rectangles indicate high expression levels of genes (encoding proteins that catalyze the indicated conversions). Yellow particles represent proteins. SOD, superoxide dismutase; GPX, glutathione peroxidase; CAT, catalase; GSR, glutathione-disulfide reductase; HSP, heat shock protein; IDH, isocitrate dehydrogenase; H_2O_2, Hydrogen peroxide; $O_2^{\cdot-}$, Superoxide anion; NADP+, nicotinamide adenine dinucleotide phosphate; NADPH, reduced nicotinamide adenine dinucleotide phosphate; GSSG, oxidized glutathione; GSH, reduced glutathione; RER, rough endoplasmic reticulum.

Fig.7

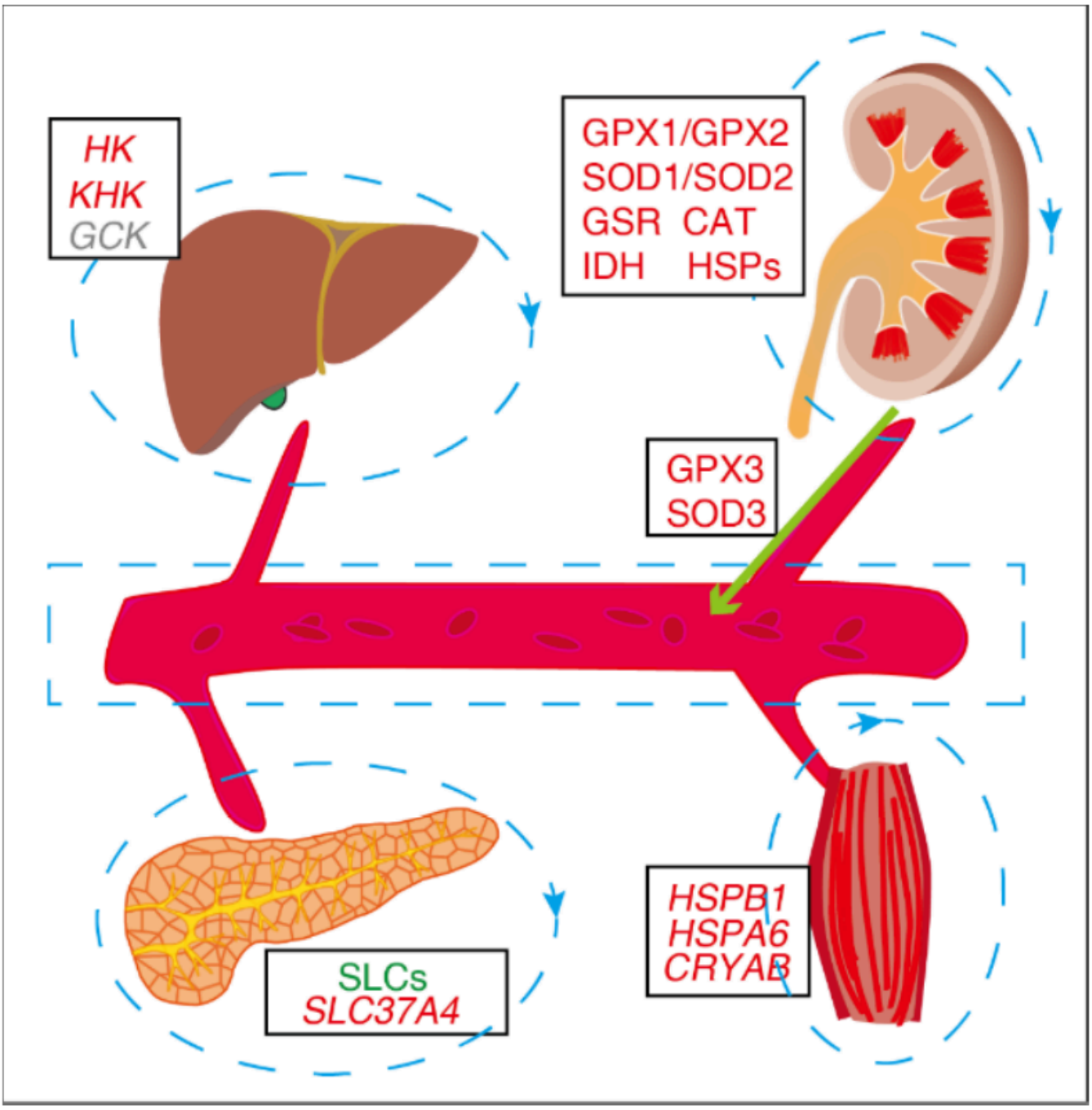


Figure 7

Diagram of High Glucose Tolerance Mechanism in camels

Liver (top left), kidney (top right), pancreas (bottom left), muscle (bottom right) and blood vessels (center) adapt to high blood sugar levels by self defense of tissue and removal of ROS in the blood. The red represents the highly expressed gene, the green represents the lowly expressed gene, and the gray represents the non-expressed gene. The green arrow represents that the proteins are secreted by the tissue into the blood.

Supplementary Files

This is a list of supplementary files associated with this preprint. Click to download.

- support.docx
- articletable.docx